NAL-TM-516
1101-200

CERN 74-21
Laboratory II
Radiation Group
9 September 1974

ORGANISATION EUROPÉENNE POUR LA RECHERCHE NUCLÉAIRE
CERN EUROPEAN ORGANIZATION FOR NUCLEAR RESEARCH

RADIATION MEASUREMENTS AROUND THE FERMILAB 300 GeV MAIN ACCELERATOR

M. Awschalom and D.D. Yovanovitch
Fermi National Accelerator Laboratory

K. Goebel, K.P. Lambert, J. Ranft*) and E. Wilson
European Organization for Nuclear Research

G E N E V A
1974

*) Visitor from Karl Marx Universität, Leipzig

RADIATION MEASUREMENTS AROUND THE FERMILAB 300 GeV MAIN ACCELERATOR

1. INTRODUCTION

When it was decided to build near Geneva a new 300 GeV accelerator (19 February, 71) the proton accelerator at Fermilab (Fermi National Accelerator Laboratory) was already nearing completion. In principle the radiation problems expected at both installations are very similar. However, the shielding problems at those installations are considerably different for the main rings and for some of the experimental areas. At both laboratories estimates for the expected stray radiation levels, dose to components and dose rate from remanent activity in the accelerator structure have been based on Monte Carlo calculations[1]. The computer codes for radiation estimates for the Fermilab accelerator were partly developed by the Neutron Physics Division of the Oak Ridge National Laboratory[2]. At CERN, most of those predictions made for the design study of the 300 GeV project were based on the computer codes developed by J. Ranft[3]. Meanwhile quite detailed calculations have been made at CERN for particular areas and components of the projected accelerator[4]. The geometries used for these calculations[5] were not too different from the geometries existing now at the Fermilab. Therefore, it was of prime interest to check the validity of the estimates against measurements. Hence in the spring of 1973 it was agreed between interested persons at CERN and Fermilab to make some simple straightforward measurements in the ring and in an experimental area. Thus, it would be possible to compare the results from dose and flux density measurements with calculations made with well developed Monte-Carlo programs. Essentially two types of measurements were made in 1973 : parasitic measurements for a period of 6 months (from 20 May 73 to 20 November 73) inside the Fermilab ring and dose and flux density measurements during a short exposure of a standard beam line magnet in a 300 GeV external proton beam in November, 1973.

All measurements were done in a collaboration of the two laboratories. The bulk of the work to arrange for the planned measurements, to position and retrieve the detectors, to monitor the beam and main ring operational conditions fell on the Fermilab team. Dose and all of the flux density measurements were performed at Fermilab (Radiation Physics Group) whereas dose measurements from CERN glass dosimeters exposed at Fermilab were measured at CERN. Calculations were done at CERN.

The measurements at the Fermilab main accelerator are representative of a real life situation for an accelerator which was developed during 1973 to reach at the end of the year respectable performance (max. intensity 7 - 8 x 10^{12} ppp at 300 GeV). Not only the intensity increased during this year, but a considerable number of machine experiments were performed and resulted in better understanding of the beam dynamics and consequently of the beam losses. The ejection efficiency has been improved considerably. Estimations made in March 73 revealed a typical ejection loss of 15 % [6a] whereas in September a figure of 8 % was given for the ejection loss. (Note added in proof, in August 1974, the extraction efficiency often run at better than 99 %). As the ring measurements covered a period of half a year, the machine conditions during these 6 months' period cannot be considered as remaining constant. However, also in a new accelerator such as the SPS at CERN a stable situation cannot be expected from the very beginning and the results obtained from the ring measurements at FNAL can therefore be considered as being typical and can be scaled for the CERN situation with the expected intensity ratio for a period of interest.

The measurements performed using a 300 GeV proton beam to interact with a thick target inside a main ring magnet will be described in another report[6b].

2. DOSE AND FLUX DENSITY MEASUREMENTS AROUND THE FERMILAB MAIN ACCELERATOR

2.1 Experimental conditions

All the measurements performed around the Fermilab main ring had to be made in parallel with normal operations. No access to the ring was possible during the scheduled running time. Thus, it was decided to make all measurements (dose and flux density measurements) with passive detectors, i.e. with integrating dosimeters and activation detectors. The number of accelerated protons, the operational mode of the accelerator and the number of protons lost at ejection was monitored during this exposure.

Eight standard positions were chosen in the ring (fig. 1) and at each position detectors were placed close to the beam element (position "up") and on the floor. The 8 places were selected according to the beam loss patterns measured via the remanent dose rate from previous operations[7] (fig. 2).

a) Measurements on the 1st (I) and 2nd (II) Lambertson magnets (LM); at this location the highest beam losses were expected (fig. 3).

b) Three locations at a typical ring magnet A-12-2 in sector A downstream the transfer hall. The locations "upstream" (III), "middle" (IV) and "downstream" (V) of the magnet were chosen to indicate the distribution along a magnet*) (fig. 4).

c) One detector location was chosen near the abort-target (VI) and near the first dump magnet (VII). In this location high losses are expected but the total amount of protons dumped with the abort system could not be monitored (figs. 5 and 6).

d) At magnet F-36-1 a detector position was chosen in an area where very little induced activity has been measured before. In this area the smallest beam losses of the whole ring were expected (quiet area (VIII)), (fig. 4).

It was important to compare the dose and flux densities measured with those calculated on the surface of the elements and on the floor as CERN plans to install electronic equipment inside special pits beneath the tunnel floor[8].

The detectors were replaced for different operational periods.

---

*) It turned out later on that the A-12-2 magnet was not a typical 300 GeV-loss point for the main ring (see below).

Altogether 7 runs were made starting on the 20th of May and ending on the 20th of November, 1973. Table I gives the operational periods, the energy of the protons and the number of accelerated and lost protons in the transfer hall. From the table we see that the operational periods were quite different in length and that the average intensity and the loss rate in the transfer hall (ejection region) varied during this half year period and varies probably also during individual runs.

2.2 The Measurements

Table II gives the detectors and their general characteristics[9] exposed in the 16 positions in the ring. They are grouped in detectors for dose measurements and detectors for flux density measurements. The dose detectors given in lines 1 and 2 were transferred to CERN after exposure and measured with a Toshiba densitometer and Beckman DB-GT spectrophotometer respectively. The other detectors were measured at FNAL by the Radiation Physics Group.

The choice of these detectors was governed by a number of practical considerations. The doses expected during the different runs and for the different locations in the ring were quite different varying over 4 orders of magnitude. For the locations with high doses glass dosimeters and hydrogen pressure dosimeters were adequate. However, the TLD dosimeters were practical only for the locations with relatively low doses. Furthermore the dosimeters used were well known and used as standard dosimeters in many similar applications at CERN, FNAL and other accelerators[10]. The detectors for measuring the flux density were chosen according to their energy response and to the half life of the radio-nuclides to be measured. During a run the intensity of the machine and the loss patterns could change. Hence, activation detectors with long half-lives such as ^{22}Na were preferable. However, activation detectors with high energy thresholds are not very sensitive and flux densities in the quiet areas could only be measured with high statistical error. The activation detectors chosen therefore represent a compromise between sensitivity, energy response and half life.

A measurement of the remanent dose rate in the FNAL ring was performed[11] before and after each run. A radiation survey Rover was used to measure the exposure rate one foot above the upper magnet surface. The Rover drew a chart giving the exposure rate as a function of position along the accelerator. From these charts one could see by how much in a given location the exposure rate from induced activity varied from one run to another. These measurements have not always been done after the same length of operation (see Table I) nor at exactly the same lapse time after machine shut-down. In order to compare the different measurements one has therefore to normalize these measurements for a given operation and cooling time[12]. Sometimes it is difficult to read from the longitudinally compressed chart the exposure rate at the precise location above the detector position. Also it should be kept in mind that the activation from a previous run may mask the activity from the last one. However, these charts are very useful to estimate the relative beam losses around the ring and they are easy to use for assessing the maximum values near the Lambertson magnet (LM) and the abort system.

2.3 The Results

The dose measurement results are given in Table IIIa - IIIe while those of the flux density in Tables IVa - IVb. For the dose measurements we can integrate over the whole 6 months, however the flux density measurements depend on the intensity during the individual runs. We can however integrate those measurements made with long-lived radio-isotopes. These integrated figures, averaged over the 7 runs, are given in column "average".

The dose results depend on the dosimetry system used. Systematically the measurements with the Toshiba glass dosimeters are lower than those made with the PDG 11 glass[13]. Both are lower than the measurements made with hydrogen pressure dosimeters. These different responses to a mixed radiation field encountered in the main ring have been found already at other accelerators in particular in the PS and in the ISR[14].

When comparing the dose measured with the expected effects on components installed in the ring one has to use the dosimeters which respond physically in a similar way as the equipment or material under irradiation. In the following we base our comparison on measurements made with Toshiba glass dosimeters keeping in mind that the measured dose is on the lower side. These dosimeters respond to charged and uncharged secondary particles and to electromagnetic interactions, they cover the effects which are also considered in the MC-calculations[15].

2.4 Comparison with calculations

In order to compare the measurements with calculations based on Monte-Carlo codes for the nucleon-meson cascade in matter we have first to estimate the losses which occur in particular components for example in the first Lambertson magnet (LM). From the experiments made in the Fermilab ring we had a record of the protons lost in the transfer hall. These measurements were performed with a 120 m long ionization chamber called "The" loss monitor (TLM)[16]. These lost protons generate along the transfer hall a pattern of induced activity. Assuming that local losses are proportional to the locally measured exposure rate from induced radioactivity, we can estimate the relative losses in the LM. Table V gives estimations based on those induced activity patterns. We find along the transfer hall about 8 individual runs between 37 and 41 % of the integrated curve. From this we would conclude that about 40 % of all protons lost in the transfer hall are lost locally in the first LM. When normalizing the dose measured underneath the LM to a total of 10^{18} p lost in the LM we estimate doses between 340 and 460 Mrad. The number of protons lost in the first LM represents about 4 % of all protons accelerated to 300 GeV. The loss in the 2nd LM is more difficult to estimate as the two activity peaks are not separated. According to the doses measured near the 2nd LM one would expect that about 1/3 of the protons lost in the 1st magnet are lost in the 2nd. However, this figure varies during the different runs as a function of the alignment of the two magnets and of the mode of operation. Also the dose on the 2nd magnet can be interpreted as a consequence of the proton losses occurring in the 1st magnet. Therefore, we have not tried to analyse in detail the dose measured on the 2nd LM. Considering the fact that the fine structure of the loss pattern is difficult to evaluate we may assume that a maximum of 80 % of all proton losses registered by the loss monitor (TLM) are lost in the 1st septum. The figure of 80 % would correspond to a total loss of about 8 % of all accelerated protons. Most probably, the true value lies between these two limits of 4% and 8%.

It is even more difficult to estimate local proton losses for the other locations where we measured the dose in the ring. The abort target which represents the 2nd largest peak in the dose measurements is not used regularly and no record is taken by any loss monitor in this area. For the magnet A-12-2 we have to envisage losses occurring after injection (8 GeV protons). From the results we see that in this area the doses at the floor are higher than the doses measured on top of the magnet. This indicates a certain asymmetry of the radiation field. Protons are injected in the transfer hall from above the main ring so that this asymmetry could be due to injected protons lost downwards.

Near magnet F-36-1 proton losses seem to be very low and it is not known whether the dose measured in this quiet area is due to 300 GeV or 8 GeV losses. In this area the radiation level on the floor is about half of the level on top of the magnet indicating that the tunnel is filled with radiation probably from losses occurring at a larger distance from the measuring location. We have therefore related the doses measured at the LM to 40 % of the losses measured with the TLM; in other areas of the ring we have related the doses to the total number of protons accelerated.

Comparison with the calculations at the LM for the whole period from the 20th May to the 20th November, 1973 are made in the following way :

21.3×10^{16} p are lost during this period in the transfer hall corresponding to 9.5 % of all the protons accelerated (225×10^{16} at 300 GeV). 40 % of the lost protons correspond to 8.5×10^{16} or 3.8 % of all protons accelerated*). The total dose measured at the first LM is 30.4 Mrad.

---

*) Bleser estimated in March 73 an average ejection efficiency of 85 % with best values up to 92 % and Yovanovitch in September 73 an ejection efficiency of 93%. After shut-down of the accelerator about 44% of all activity in the ring is found in the transfer hall; we estimate for 4 individual runs this figure to be between 37 and 41%.

From this we obtain 3.6×10^{-10} rad/p or 1.8×10^{-4} GeV/p.

For the same geometry (see figure 7) Monte Carlo calculations have been performed using the program MAGKA. At the point of interest (18 cm below the beam line) a maximum energy deposition of 1×10^{-4} GeV/p is found. This compares quite well with the measured value given above assuming a local loss of 40 % at the 1st LM. For a local loss of 75 % at the LM we would exactly obtain 1×10^{-4} GeV/p from the measurements. We can conclude that the agreement is excellent when we take into consideration that the proton losses at the LM cannot be estimated better than within a factor of 2 (40 % to 80 % of the TLM monitor).

2.5 Exposure Rate Measurements in the Ring

Before and after each run exposure rate measurements in the ring were performed with a Rover carrying a GM detector assembly. The exposure rate measured 1 foot above the beam elements when driving the Rover around the ring is recorded on a chart. On this chart the distribution of exposure rate due to induced activity is given in a logarithmic scale (see fig. 2.). When examining this exposure rate pattern one finds that typical decay lengths from high peaks are the same all over the ring. As the exposure rate patterns approximately reflect the beam loss patterns during the individual runs one could in principle estimate the losses in each particular element of the accelerator. However, losses in the ring occur at all energies during the accelerating cycle. Typically, an important loss occurs during injection (30 - 50 % of all protons injected at 8 GeV are lost during the first few turns). Important losses (between 5 - 15%) occur during ejection. Depending on the operation, losses occur also in the beam abort system. It has been proposed to assume that the production of induced activity is directly proportional to the beam energy deposited[17]. From the exposure rate patterns we can therefore make conclusions about the beam loss patterns only if we make assumptions about the energy of protons lost in a particular region. It has been proposed to assume that all losses in the rest of the ring are due to 8 GeV protons[18]. From the exposure rate distribution in the transfer hall we can estimate the losses in an individual element compared to the total number of protons lost as recorded by the transfer hall monitor (TLM). We have examined the loss patterns of 4 individual runs, namely 1,2,3,5. According to the integral: "(mR/hr) x m" we estimate losses in the first Lambertson Magnet to be in all runs about 40 %. We have used the highest peak of the exposure rate curve (first LM) to estimate the exposure rate gained during 4 runs. This can be done when comparing the exposure rate measured before and after the run. However, we have to assume a typical time dependence of the exposure rate with respect to the irradiation time T and the cooling time t. It has been found at the present CERN accelerators that the exposure rate dependence following log $\frac{T+t}{t}$ agrees well with many measurements[19]).

Table VI gives the results of the corrections applied to the measured exposure rate peaks. In order to compare the exposure rate with star density calculations we have normalized all peaks to 30 days of irradiation and 1 day of cooling. The numbers are given in the column DR (30,1).

The average loss rate of protons in the first LM has been estimated by using the number of protons lost (TLM) averaged over the duration of the run and applying the above mentioned factor 0.4. The results of these calculations show that in average the dose rate at 1 ft from the LM is about 0.64 R/h for 10^{10} protons lost/second (Table VI).

These results can now be compared with calculations using the program MAGKA. For a steel cylinder (representing the LM) of 13 cm outer radius and with a central hole of 8 cm diameter, we obtain on the surface of this cylinder a star density of 10^{-4} stars/cm^3/p (see fig. 7). Applying the factor $\omega = 1.2 \times 10^{-6} \frac{\text{rem/h}}{\text{star/cm}^3\text{/s}}$ we obtain on the surface of the LM a dose rate of 1.2 rem/h for 10^{10} protons/s. This surface dose rate has to be scaled to the measuring distance about 50 cm from the beam axis. When assuming 1/r dependence which has been found to be reasonable for such geometries we would expect a dose rate of about 300 mrem/h. This is about a factor 2 lower than the above measured value. However, the assumption we made for the number of protons lost in the LM may be too low. In fact it represents only 3.8 % of all accelerated protons. For a loss of 8% of all accelerated protons at the LM we would have perfect agreement with our calculated number. On the other hand we cannot claim from our estimations a certainty better than a factor 2 and therefore also the higher value is in satisfactory agreement with our estimations : (DR(30,1) at 50 cm from beam 300-650 mrem/h for 10^{10} protons/s. lost locally).

For the thin septum of the CERN SPS it was assumed that 4 to 6 x 10^{10} p/s would be lost. With this number one would expect at the FNAL Lambertson Magnet a dose rate between 1.2 and 4 rem/h at 50 cm distance. The star density expected at the SPS ejection elements are between 1.2 to 1.8 x 10^{-4} stars/cm^3/p[20]. With (4-6) x 10^{10} protons lost per second we obtain a surface exposure rate between 5 and 13 R/hour. A dose rate of 3-6 R/h was given[21] near the tank surface of the ejection elements, this compares well with the estimations made for the LM at 50 cm distance. Values of this order have also to be expected at the LM when the FNAL accelerator will work with a maximum intensity of 5 x 10^{13} ppp and a ejection efficiency of 98 %[21].

2.6 Comparison of Dose and Flux Densities in the NAL Ring

The flux densities measured during the 7 runs in the 16 positions in the Fermilab ring (see Table IV) can be used to estimate the dose during operation. At CERN such estimations had been made[22] using empirical factors for the flux density to dose conversion :

$$D = (6\cdot 10^{-8}\ \phi_{^{32}P} + 5\cdot 10^{-8}\ \phi_{^{22}Na})\ \text{rad}$$

By calculating the dose using $D = 10^{-7}\cdot\phi_{^{22}Na}$ Rad, (assumption : $\phi_{^{32}P} / \phi_{^{22}Na} \sim 1$) we obtain for the different positions the doses given in Table VII. In this table we have repeated the dose measurements made with the CERN glass dosimeters. The agreement is satisfactory. We may therefore conclude that at some distance from the beam axis the dose in the NAL accelerator is produced by similar radiation fields as in the CPS. It should however be kept in mind that more than half of the dose near to the beam is due to electromagnetic interactions at 300 GeV[23]. This part of the dose is not measured by the activation detector. The empirical factor given above should therefore only be used outside the main electromagnetic cascade.

3. CONCLUSIONS

This experiment is the first systematic dose and flux density measurements in this new energy range of 200/300 GeV. A few remarks are at hand :

i) The dose measurements in the ring show large variations in the longitudinal distribution spanning over more than 4 orders of magnitude and are very similar to those found in the CPS, the AGS or the Serpukhov accelerator.

ii) The radial distribution measured at two points near the elements and on the tunnel floor changes drastically. The ratio Dos Magnet / Dose on the floor is 20-30 near a high loss area, the Lambertson magnets or the Abort-system and become 1 near the magnets following injection. We may conclude : the higher the loss the more one gains by installing equipment near or underneath the tunnel floor.

iii) The doses measured in the FNAL ring during a half year period agree with estimations based on present experience at lower energy and are in accordance with assumptions for beam losses in the SPS, e.g. 3.8% losses at the first Lambertson magnet NAL, 3.5% losses assumed as maximum loss for the ES of the SPS.

iv) For locations and situations for which beam loss estimates can be made within reasonable limits the calculations agree quite well with the dose measurements.

v) The simplified geometry used in the calculation reveals results which agree well with the doses found at the Lambertson Magnet showing that the details of the geometry do not influence the results appreciably beyond the normally accepted error margin of a factor 2-3.

vi) When applying "star density-activity" conversion factors as found for lower energies, the exposure rate estimates based on star density are in good agreement with the measurements in the ring.

All evidence we have from the measurements made at 200-300 GeV primary proton energy at FNAL give credibility to the MC-calculations used for estimating doses at the SPS. This is important also for the many other applications of these computer programs e.g. shielding assessment, target heating, etc. The comparisons of dose estimates with measurements of dose and fluence are rather satisfactory. They prove that the properties of the dose producing particles near the 300 GeV accelerator are not too different from the radiation spectra around smaller accelerators, otherwise the conversion factor for 200 and 300 GeV should be different from the one used at 20 GeV.

The different comparisons taught us that the calculated results are in the right order of magnitude. The exposure rates given for the SPS ring, ejection area and target stations must therefore be considered as experimentally confirmed.

ACKNOWLEDGEMENTS

The authors would like to thank the Fermilab operational team and the experimental area group for their assistance in scheduling and making the measurements. Thanks are also due to E. Smith for preparing the activation + dosimeter packages and reading the hydrogen dosimeters, to J. Baldwin for reading the aluminium and copper disks, and Mary-Ann Ogg for reading the thermoluminescent dosimeters.

REFERENCES

1) Radiation problems encountered in the design of multi-GeV research facilities.
Editor : K. Goebel
Chapter II : J. Ranft, "The interaction of protons in machine components and beam loss distribution".
Chapter III : E. Freytag and J. Ranft, "Hadronic and electronic cascades".

2) R.G. Alsmiller Jr.,
Electromagnetic and nuclear cascade calculations and their applications in shielding and dosimetry.
Proc. 2nd Int. Conf. on Accelerator Dosimetry and Experience Stanford 1969, CONF.-691101, page 253.

3) J. Ranft,
Monte Carlo calculations of hadronic cascades of high energy.
First European Conference on Computational Physics, Genève, April 1972.

4) M. Ellefsplass and J.T. Routti,
Estimates of radiation doses to the extraction components based on hadron cascade calculations. /LABII-RA/Note/72-9.

K. Goebel, J. Ranft, J.T. Routti and M. Van de Voorde,
Estimates of radiation doses to machine components in normal areas of the main ring. / LABII-RA/72-1/ (March 6, 1972).

M. Ellefsplass, K. Goebel, J. Ranft and H. Schönbacher,
Estimations of dose to components and dose rates from remanent activity in the West Target area and in the neutrino cave.
LABII-RA/74-1.

5) J. Ranft and J.T. Routti,
FLUKA and MAGKA Monte Carlo programs for calculating nucleon-meson cascades in cylindrical geometries.
LABII-RA/71-4 (24.11.1971).

J. Ranft,
Estimation of radiation problems around high energy accelerators using calculations of the hadronic cascade in matter.
Particle accelerators, 1972, vol. 3 pp 129-161.

6a) E.J. Bleser,
"The" Loss Monitor Calibration (EXP-37)
Personal communications, March 1973.

6b) M. Awschalom et. al.
CERN/NAL report to be prepared.

7) R.E. Shafer and D.D. Yovanovitch,
Radiation survey vehicle for the NAL main ring, Nat. Acc. Lab., Batavia, USA.

8) S. Battisti, R. Bossart, L. Burnod, E. Marcarini, H. Schönbacher and M. Van de Voorde,
Radiation damage of electronic components / LABII-RA/72-10, October, 1972.

9) S. Charalambus, J. Dutrannois and K. Goebel,
Particle flux measurements with activation detectors, /CERN DI/HP/90 (14.7.1966).

K.P. Lambert and M. Van de Voorde,
High radiation dose luminescent and optical dosimetry system. /CERN ISR-MA/73-36/ (1973).

10) J.T. Routti and M. Van de Voorde,
Intercomparison of high dose dosimeters in accelerator radiation fields.
Nucl. Instr. Meth. 99 563-571 (1972).

11) Personal communications, D.D. Yovanovitch (1973)
see also D.D. Yovanovitch and R.E. Shafer IEEE NS20, 499 (1973).

12) A.M. Sullivan and T.R. Overton,
Time variation of the dose rate from radioactivity induced in high energy particle accelerators, Health Physics 11, 1101 (1965).

13) K.P. Lambert, H. Schönbacher and M. Van de Voorde,
High radiation dose dosimetry systems / CERN LABII-RA/PP/74-3/ (17.6.1974).

14) K. Goebel and M. Nielsen,
Routine flux density and dose rate measurements near the CPS-vacuum chamber. /CERN HP-69-69 (Febr. 1969).

M. Höfert, M. Nielsen and J.M. Hanon,
Predictions of future radiation levels from induced radioactivity around the proton synchrotron and in regions near external targets in view of higher machine intensities / CERN HP-73-124 (16.4.1973).

K.P. Lambert, M. Van de Voorde, F. Rohner, M. Höfert and M. Nielsen,
Radiation dose measurements around the CPS ring during the 1972 and 1973 running period. (CERN - in preparation).

15) J. Ranft,
Monte Carlo calculation of energy deposition by the nucleon-meson cascade and total absorption - Nuclear cascade counters (TANC).
Nucl. Instr. Meth. 81 29 (1970).

16) Fred Hornstra,
"The" Loss Monitor, Personal communication.

17) M. Awschalom,
FNAL Design Report (1968).

18) D. Yovanovitch
Induced activity in the main ring NAL, sept. 1973.
personal communication.

19) A.H. Sullivan,
An approximate relation for the estimation of the dose-rate from radioactivity induced in high-energy particle accelerators.
CERN HP-71-96 (1971).

20) M. Ellefsplass and J.T. Routti,
Estimates of radiation doses to the extraction components based on hadron cascade calculations.
LABII-RA/Note/72-9 (2.5.1972).

21) K. Goebel, J. Ranft, J.T. Routti and G.R. Stevenson,
Estimation of remanent dose rates from induced activity in the SPS ring and target areas.
CERN LABII-RA/73-5 (24.7.73).

22) M. Höfert,
Dosimeter response in the high energy radiation field around the CERN proton synchrotron.
CERN DI/HP/162 (14.11.1972).

23) J. Ranft,
Radiation doses on synchrotron magnets and around target stations.
TUL-39 (1970), Technische Universität, Leipzig.

Table I : Protons accelerated and protons lost in NAL Transfer Hall (TH)

Run	period	days	protons accel. to 200 GeV 10^{16}	protons accel. to 300 GeV 10^{16}	protons lost (TLM) at 200 GeV 10^{16}	protons lost (TLM) at 300 GeV 10^{16}	ejection losses %	average intensity acc/sec 10^{10}	average intensity lost/sec 10^{10}
1	20.V - 28.V	9		6.32		1.33	21 %	9.14	1.92
2	28.V - 6.VI	10		16.57		1.50	9.1 %	19.18	1.74
3	12.VI - 25.VI	12		7.46		0.84	11.3 %	7.20	0.89
4	5.VII - 11.VII	7		6.00		0.99	16.5 %	9.92	1.64
5	11.VII - 27.VIII	48	13,86	(11.32)	1.04	(0.85)	7.5 %	17.90	2.08
				62.90		7.77	12.4 %		
6.	27.VIII - 9.IX	14	34,40	(28.10)	2.45	(1.99)	7.1 %	23.23	1.65
	23.IX - 12.X	20		20.30		2.03	10.0 %	11.74	1.17
7.	15.X - 22.X	8							
	28.X - 20 XI	24		66.40		4.01	6.0 %	24.0	1.37
1-7	20.V - 20.XI	152						17.1	1.62
	half year av.	183		225		21.3	9.5%	14.2	1.35

Table II

Dosimeter	Dimensions	Dose Range (rad)	Read-out	Calibration	Use
Toshiba FD-R1-1	6 x 1 ∅	$1 - 5 \times 10^8$	Photoluminescent	^{60}Co-γ	standard CERN radiation dosimeters for high doses
Schott glass PDG-11	36 x 12 x 5	$1.6\times10^4 - 5\times10^5$	Spectrophotometric	^{60}Co-γ	
	36 x 12 x 1.5	$1.4\times10^5 - 2\times10^7$			
H_2 - pressure (RHEL)		$10^4 - 10^9$	Monometric	^{60}Co-γ	
TLD-NAL		$0.1 - 10^4$	Thermoluminescent	^{60}Co-γ	

Activation detector		Radionuclide measured (half life)	Measurements γ-spectrometer	Reaction	Threshold/cross sect. MeV	(mb)
Aluminium disks	1.27 mm thick	^{22}Na(2.64y)	γ:1.39 MeV, 0,511 MeV	$^{27}Al(x;x2p3n)^{22}Na$	40	15
	51.2 mm ∅	^{24}Na (15 h)	γ:2,543 MeV, 1,38 MeV	$^{27}Al(n;2n2p)\ ^{24}Na$	6.2	120
Copper disks	1.02 mm thick	^{54}Mn (315 d)	γ:0.82 MeV	Cu(spall) ^{54}Mn	60	8
	3.84 mm ∅					

Table IIIa : TOSHIBA RPL

	Pos. No	Run No		1	2	3	4	5	6	7	average
				20.V - 28.V	28.V - 6.VI	12.VI - 25.VI	5.VII - 11.VII	11.VII - 27.VIII	27.VIII - 12.X	15.X - 20.XI	20.V - 20.XI
				Dose (rad) for 10^{18} lost protons at the Lambertson magnet (0.40 of TLM)							
LAMBERTSON MAGNETS	I	1st	up	4.32 E8	3.33 E8	3.28 E8	3.79 E8	4.64 E8	1.88 E8	2.80 E8	3.42 E8
			floor	3.74 E7	3.33 E7	3.58 E7	2.53 E7	1.71 E7	3.14 E7	2.49 E7	2.94 E7
	II	2nd	up	1.35 E8	1.66 E8	2.98 E8	2.27 E8	1.30 E8	1.50 E8	1.43 E8	1.78 E8
			floor	3.57 E7	1.66 E7	2.98 E7	2.53 E7	1.45 E7	2.26 E7	2.24 E7	2.38 E7
				Dose (rad) for $4\cdot10^{19}$ accelerated protons (300 GeV)							
RING MAGNET A-12-2	III	upstream	up	1.32 E7	4.82 E6	1.63 E7	2.67 E7	5.95 E6	8.46 E6	5.43 E6	1.15 E7
			floor	2.85 E7	2.04 E7	3.94 E7	2.87 E7	2.70 E7	8.46 E6	7.24 E6	2.27 E7
	IV	middle	up	7.60 E6	5.78 E6	6.76 E6	8.00 E6	5.41 E6	8.46 E6	2.71 E6	6.37 E6
			floor	1.58 E8	1.20 E7	1.35 E7	1.60 E7	5.95 E6	8.46 E6	6.03 E6	3.12 E7
	V	downstream	up	6.01 E6	4.10 E6	6.76 E6	5.67 E6	5.95 E6	8.46 E6	2.17 E6	5.58 E6
			floor	1.20 E7	7.47 E6	1.01 E7	1.20 E7	2.70 E7	8.46 E6	6.03 E6	1.18 E7
ABORT SYSTEM	VI	target	up	6.33 E8	5.78 E8	6.20 E8	4.80 E8	1.89 E8	7.44 E7	-	-
			floor	7.60 E7	2.41 E7	5.63 E7	6.67 E7	5.41 E6	8.46 E6	2.41 E7	3.72 E7
	VII	dump.magnet	up	6.32 E7	1.11 E8	9.57 E7	2.40 E8	2.70 E7	8.46 E6	3.50 E7	8.28 E7
			floor	7.60 E7	2.41 E7	5.63 E7	6.67 E7	1.08 E7	8.46 E6	1.21 E7	3.62 E7
ING AGNET	VIII	F-36-1	up	2.85 E5	7.23 E4	6.20 E4	1.07 E5	8.66 E4	2.88 E5	3.32 E4	1.33 E5
			floor	1.27 E5	1.81 E4	4.22 E4	5.00 E4	3.24 E4	-	1.33 E4	-

Table IIIb : PDG-11 (CERN GLASS)

	Pos. No	Run No		1	2	3	4	5	6	7	average
				20.V - 28.V	28.V - 6.VI	12.VI - 25.VI	5.VII - 11.VII	11.VII - 27.VIII	27.VIII - 12.X	15.X - 20.XI	20.V - 20.XI
				Dose (rad) for 10^{18} lost protons at the Lambertson magnet (0.40 of TLM)							
LAMBERTSON MAGNETS	I	1st	(up	6.58 E8	5.33 E8	6.87 E8	5.83 E8	3.49 E8	2.51 E8	7.48 E8	5.44 E8
			floor	-	-	-	-	-	-	-	-
	II	2nd	(up	4.32 E8	2.83 E8	7.77 E8	5.57 E8	1.74 E8	2.51 E8	3.55 E8	4.04 E8
			floor	-	-	-	-	-	-	-	-
				Dose (rad) for $4 \cdot 10^{19}$ accelerated protons (300 GeV)							
RING MAGNET -12-2	III	upstream	(up	2.03 E7	1.08 E7	1.91 E7	2.67 E7	4.87 E6	1.18 E7	4.46 E6	1.39 E7
			floor	-	-	-	-	-	-	-	-
	IV	middle	(up	1.77 E7	7.71 E6	1.58 E7	<1.87 E7	4.60 E6	4.48 E6	2.41 E6	1.01 E7
			floor	-	-	-	-	-	-	-	-
	V	downstream	(up	1.77 E7	6.75 E6	<1.58 E7	<1.87 E7	2.43 E6	3.81 E6	2.17 E6	9.60 E6
			floor	-	-	-	-	-	-	-	-
BORT YSTEM	VI	target	(up	1.01 E9	8.19 E8	1.18 E9	1.00 E9	2.71 E8	1.18 E8	-	-
			floor	-	-	-	-	-	-	-	-
	VII	dump.mag.	(up	1.71 E8	1.52 E8	1.13 E8	2.67 E8	5.41 E7	1.18 E7	6.03 E7	1.18 E8
			floor	-	-	-	-	-	-	-	-
ING AGNET	VIII	F-36-1	(up	-	-	-	-	-	-	-	-
			floor	-	-	-	-	-	-	-	-

Table IIIc : H_2-DOSIMETERS

	Pos. No	Run No		1	2	3	4	5	6	7	average
				20.V - 28.V	28.V - 6.VI	12.VI - 25.VI	5.VII - 11.VII	11.VII - 27.VIII	27.VIII - 12.X	15.X - 20.XI	20.V - 20.XI
				Dose (rad) for 10^{18} lost protons at the Lambertson magnet (0.40 of TLM)							
MBERTSON GNETS	I	1st	up	1.11 E9	1.13 E9	8.06 E8	5.32 E8	1.46 E9	4.46 E8	8.25 E8	9.01 E8
			floor	-	3.17 E7	-	-	-	6.28 E7	4.04 E7	-
	II	2nd	up	2.59 E8	2.55 E8	1.79 E8	-	5.06 E9	3.70 E8	3.97 E8	-
			floor	-	2.33 E7	-	-	-	1.88 E7	4.04 E7	-
				Dose (rad) for $4 \cdot 10^{19}$ accelerated protons (300 GeV)							
	III	upstream	up	-	-	-	-	1.08 E7	2.54 E7	1.75 E7	-
NG GNET 12-2			floor	-	1.20 E7	-	3.60 E9	1.62 E7	3.38 E7	1.15 E7	-
	IV	middle	up	-	3.37 E7	-	-	1.08 E7	1.69 E7	1.15 E7	-
			floor	-	-	-	-	2.16 E7	1.69 E7	5.73 E6	-
	V	downstream	up	-	-	-	-	5.41 E6	1.69 E7	5.73 E6	-
			floor	-	1.20 E7	-	-	1.08 E7	2.54 E7	5.73 E6	-
	VI	target	up	1.07 E9	1.32 E9	3.94 E8	-	4.54 E8	1.27 E8	8.42 E8	-
RT TEM			floor	-	3.37 E7	-	-	1.62 E7	3.38 E7	4.30 E7	-
	VII	dump.mag.	up	1.90 E8	2.17 E6	-	-	-	3.38 E7	8.02 E7	-
			floor	-	-	-	-	-	8.46 E6	2.30 E7	-
IET	VIII	F-36-1	up	-	-	-	-	5.41 E6	1.69 E7	2.90 E6	-
			floor	-	1.20 E7	-	-	2.16 E7	-	5.73 E6	-

Table IIId : TLD-600

	Pos. No	Run No		1	2	3	4	5	6	7	average
				20.V - 28.V	28.V - 6.VI	12.VI - 25.VI	5.VII - 11.VII	11.VII - 27.VIII	27.VIII - 12.X	15.X - 20.XI	20.V - 20.XI
				Dose (rad) for 10^{18} lost protons at the Lambertson magnet (0.40 of TLM)							
	I	1st	(up	-	-	-	-	-	-	-	-
AMBERTSON AGNETS			floor	>2.82 E6	>4.5 E6**	>1.11 E7**	7.09 E7	>1.05 E6**	>4.96 E6**	>6.85 E6**	>1.45 E7
	II	2nd	(up	-	-	-	-	-	-	-	-
			floor	-	> 6.70 E6**	>1.02 E7**	7.72 E7	>1.63 E6**	>6.97 E6**	>7.48 E6**	-
				Dose (rad) for $4 \cdot 10^{19}$ accelerated protons (300 GeV)							
	III	upstream	(up	-	-	-	-	-	-	-	-
			floor	3.8 E6	8.19 E6	-	5.93 E7	>1.08 E7**	>1.34 E7**	1.03 E7	
ING AGNET -12-2	IV	middle	(up	-	-	-	-	-	-	-	-
			floor	5.0 E6	6.50 E6	6.76 E6	5.93 E7	9.74 E6	>1.07 E7**	8.45 E6	>1.51 E7
	V	downstream	(up	-	-	-	-	-	-	-	-
			floor	2.66 E6	7.47 E6	6.76 E6	3.07 E7	1.04 E7	1.40 E7	6.03 E6	1.11 E7
	VI	target	(up	-	-	-	-	-	-	-	-
BORT YSTEM			floor	8.23 E6	1.06 E7	1.69 E7	1.20 E8	4.0 E6	1.08 E7	>1.21 E7**	>2.47 E7
	VII	dump.mag.	(up	-	-	-	-	-	-	-	-
			floor	8.87 E6	1.04 E7	1.35 E7	2.00 E8	>1.03 E7**	1.09 E7	>1.03 E7	>3.77 E7
ING AGNET	VIII	F-36-1	(up	-	-	8.45 E4	1.33 E5	9.74 E4	3.05 E5	2.71 E4	-
			floor	4.30 E5	8.67 E4	7.89 E4	1.60 E5	>7.03 E6**	-	3.92 E4	-

* turned amber
** turned yellow

Table IIIe : TLD-700

	Pos. No	Run No		1	2	3	4	5	6	7	average
				20.V - 28.V	28.V - 6.VI	12.VI - 25.VI	5.VII - 11.VII	11.VII - 27.VIII	27.VIII - 12.X	15.X - 20.XI	20.V - 20.XI
				Dose (rad) for 10^{18} lost protons at the Lambertson magnet (0.40 of TLM)							
BERTSON NETS	I	1st	up	-	-	-	-	-	-	-	-
			floor	2.82 E6	4.12 E6	5.67 E6	4.48 E7	>1.15 E6**	2.56 E5	2.31 E7	>1.17 E7
	II	2nd	up	-	-	-	-	-	-	-	-
			floor	-	6.33 E6	5.67 E6	4.58 E7	>1.05 E6**	2.54 E5	>1.81 E7	-
				Dose (rad) for $4 \cdot 10^{19}$ accelerated protons (300 GeV)							
G NET 2-2	III	upstream	up	-	-	-	-	-	-	-	-
			floor	2.15 E6	4.10 E6	-	3.33 E7	1.55 E7	2.94 E7	1.39 E7	-
	IV	middle	up	-	-	-	-	-	-	-	-
			floor	2.34 E6	2.89 E6	3.21 E6	1.73 E7	1.04 E7	2.00 E7	9.05 E6	9.31 E6
	V	downstream	up	-	-	-	-	-	-	-	-
			floor	1.08 E6	-	2.98 E6	8.67 E6	6.82 E6	1.18 E7	6.64 E6	-
RT EM	VI	target	up	-	-	-	-	-	-	-	-
			floor	6.27 E6	9.40 E6	1.01 E7	7.87 E7	4.33 E3	1.55 E7	>2.59 E7	>2.07 E7
	VII	dump.mag.	up	-	-	-	-	-	-	-	-
			floor	5.19 E6	8.91 E6	1.07 E7	1.30 E8	>2.10 E7**	5.16 E6	2.29 E7	>2.91 E7
ET	VIII	F-36-1	up	-	-	1.69 E4	2.00 E4	2.81 E4	1.27 E5	7.84 E3	-
			floor	1.71 E4	3.13 E3	6.76 E3	6.00 E3	>1.95 E7**	-	2.41 E3	-

* turned amber
** turned yellow

Table IVa : ^{22}Na ACTIVITIES

	Pos. No	Run No		1	2	3	4	5	6	7	average
				20.V - 28.V	28.V - 6.VI	12.VI - 25.VI	5.VII - 11.VII	11.VII - 27.VIII	27.VIII - 12.X	15.X - 20.XI	20.V - 20.XI
				nCi g^{-1} for 10^{18} lost protons at the Lambertson magnet (0.40 of TLM)							
MBERTSON GNETS	I	1st	up	1.35 E3	1.05 E3	8.06 E2	8.97 E2	9.90 E2	4.34 E2	8.33 E2	9.08 E2
			floor	5.07 E1	4.33 E1	4.48 E1	3.55 E1	4.18 E1	-	-	-
	II	2nd	up	2.07 E2	2.50 E2	3.82 E2	3.21 E2	2.80 E2	3.19 E2	3.32 E2	2.98 E2
			floor	3.38 E1	3.50 E1	3.58 E1	3.29 E1	2.74 E1	3.05 E1	2.90 E1	3.20 E1
				nCi g^{-1} for $4 \cdot 10^{19}$ accelerated protons (300 GeV)							
NG GNET 12-2	III	upstream	up	2.41 E1	1.93 E1	1.68 E1	2.67 E1	6.76 E0	2.31 E1	4.22 E0	1.72 E1
			floor	1.77 E1	7.23 E0	3.38 E1	2.00 E1	5.15 E0	1.36 E1	4.34 E0	1.45 E1
	IV	middle	up	-	9.64 E0	<5.63 E0	<6.67 E0	3.79 E0	1.11 E2	1.75 E0	-
			floor	1.14 E1	7.23 E0	5.63 E1	1.33 E0	3.18 E0	1.21 E1	3.50 E0	1.35 E1
	V	downstream	up	-	4.82 E0	1.13 E1	<6.67 E0	2.11 E0	7.66 E0	1.54 E0	-
			floor	-	4.82 E0	1.13 E1	<6.67 E0	2.73 E0	5.07 E0	2.11 Eo	-
IRT STEM	VI	target	up	1.11 E3	6.50 E2	6.57 E2	7.47 E2	2.90 E2	1.00 E2	5.88 E2	5.91 E2
			floor	3.35 E1	2.65 E1	5.63 E1	2.67 E1	5.41 E-2	6.21 E0	2.19 E1	2.45 E1
	VII	dump.mag.	up	1.90 E2	1.45 E2	1.35 E2	2.80 E2	6.13 E1	1.74 E1	6.29 E1	1.27 E2
			floor	2.78 E1	2.65 E1	3.38 E1	4.00 E1	1.11 E1	3.13 E0	1.00 E1	2.17 E1
IG NET	VIII	F-36-1	up	-	<2.41 E0	<5.63 E0	<6.67 E0	1.90 E-1	2.03 E0	5.00 E-1	-
			floor	-	<2.41 E0	2.82 E1	<6.67 E0	8.92 E0	-	3.00 E-1	-

Table IVb : ^{54}Mn ACTIVITIES

	Pos. No	Run No		1	2	3	4	5	6	7	average
				20.V - 28.V	28.V - 6.VI	12.VI - 25.VI	5.VII - 11.VII	11.VII - 27.VIII	27.VIII - 12.X	15.X - 20.XI	20.V - 20.XI
				nCi g^{-1} for 10^{18} lost protons at the Lambertson magnet (0.40 of TLM)							
LAMBERTSON MAGNETS	I	1st	up	1.65 E3	1.32 E3	1.17 E3	1.26 E3	1.17 E3	3.64 E2	9.10 E2	1.12 E3
			floor	5.26 E1	4.17 E1	1.49 E1	3.55 E1	3.72 E1	4.45 E1	3.22 E1	3.70 E1
	II	2nd	up	2.63 E2	3.17 E2	4.70 E2	2.12 E2	3.52 E2	3.83 E2	3.89 E2	3.41 E2
			floor	6.95 E1	4.17 E1	1.91 E1	3.80 E1	3.14 E1	3.55 E1	3.15 E1	3.81 E1
				nCi g^{-1} for $4\cdot10^{19}$ accelerated protons (300 GeV)							
RING MAGNET A-12-2	III	upstream	up	1.96 E1	2.05 E1	1.13 E1	2.00 E1	9.14 E0	2.18 E1	3.98 E0	1.51 E0
			floor	1.96 E1	1.16 E1	1.13 E1	2.00 E1	6.55 E0	1.73 E1	5.07 E0	1.30 E1
	IV	middle	up	-	3.85 E0	<5.63 E0	6.67 E0	2.98 E0	6.64 E0	1.99 E0	-
			floor	1.08 E1	7.23 E0	<5.63 E0	6.67 E0	5.30 E0	1.06 E1	3.74 E0	<7.14 E0
	V	downstream	up	-	6.75 E0	<5.63 E0	<6.67 E0	2.60 E0	3.79 E0	1.45 E0	-
			floor	-	4.10 E0	<5.63 E0	<6.67 E0	3.30 E0	6.18 E0	2.65 E0	-
ABORT SYSTEM	VI	target	up	1.65 E3	1.08 E3	4.84 E2	1.28 E3	4.10 E2	1.31 E2	8.56 E2	8.41 E2
			floor	3.60 E1	3.37 E1	1.69 E1	3.33 E1	4.9 E-2	7.33 E0	2.77 E1	2.22 E1
	VII	dump.mag.	up	2.28 E2	1.52 E2	1.40 E2	3.06 E2	6.34 E1	1.60 E1	6.63 E1	1.38 E2
			floor	4.05 E1	3.13 E1	1.69 E1	4.67 E1	1.4 E1	2.87 E0	1.19 E1	2.34 E1
RING MAGNET	VIII	F-36-1	up	<1.89 E0	<0.72 E0	<5.63 E0	<6.67 E0	1.6 E-1	4.50 E-1	1.15 E-1	<2.22 E0
			floor	-	<0.72 E0	<5.63 E0	<6.67 E0	9.36 E0	-	7.84 E-2	-

Table V : PROTON LOSSES OCCURRING AT 1st LAMBERTSON MAGNET (estimated from remanent exposure rate patterns)

	Run 1	2	3	4
Transfer hall mR/h x meter	11000	19000	9100	22900
Protons lost/run Transfer hall	1.33×10^{16}	1.5×10^{16}	0.84×10^{16}	8.62×10^{16}
First L. Magnet mR/h x meter	4200	7000	3500	9500
% of activity in L. Magnet	40 %	37 %	39 %	41 %
% of losses at LM per accel. protons	8.4 %	3.4 %	4.4 %	4.8 %

40 % of transfer hall activity is in the peak produced by the first Lambertson Magnet.

$$\frac{\text{Protons lost/run in the transfer hall x 0.40}}{\text{number of accelerated protons}} = 3.8\ \%\ \text{for all 7 runs}$$

Table VI: Development of Fxposure Rate at the 1st Lambertson Magnet

(corrections based on DR ~ $\log(\frac{T+t}{t})$)

run	date of meas.	exp. rate measured	200 mR/h corrected	420 mR/h corrected	700 mR/h corrected	350 mR/h corrected	400 mR/h corrected	ΔDR	DR (30,1)
I	20.5	200							
	28.5	420	-85					335	352
II	6.6	700	-49	-105				545	412
III	25.6	350	-36	- 56	-51			207	270
IV	11.7	(400)	not measured, estimated						
V	28.8	950	-23	- 23	-14	-15	-47	828	527

DR(30.1) mR/h	TLM losses/sec	0.4 TLM/sec Lamb. Mag.	DR(30,1) 10^{10} p/s Lamb.M.	Average 40 % of TLM)
I 352	1.92 10^{10}	0.77 10^{10}	0.45 R /h	
II 412	1.74 10^{10}	0.64 10^{10}	0.64 R /h	$\frac{0.64 \text{ rem/h}}{10^{10} \text{ p/sec of LM}}$
III 271	0.81 10^{10}	0.32 10^{10}	0.84 R /h	
V 527	2.08 10^{10}	0.85 10^{10}	0.62 R /h	

Average FNAL losses (1973): 0.40 x 1.62 10^{10} = 0.65 10^{10} p/sec : 420 mR/h

Expected ejection losses : $8\cdot10^{12}$x0.01x0.4 = 3.20 10^{10} p/sec : 2000 mR/h DR(30,1) at 1 foot

Position	1 Σ Ø ^{22}Na × 10^{14}	2 Dose(Ø)^{22}Na Mrad	3 Toshiba Mrad	Ratio $\frac{UP}{DN}$ (Toshiba)	Ratio $\frac{2}{3}$
I UP	101.8	1018.0	386.4	12.9	2.6
DN	4.3	43.0	29.8		1.4
II UP	29.8	298.0	178.5	7.5	1.6
DN	3.2	32.0	23.8		1.3
III UP	1.7	17.0	11.5	0.5	1.5
DN	1.5	15.0	22.7		0.7
IV UP	2.3	23.0	6.2	0.6	3.7
DN	1.4	14.0	10.2		1.4
V UP	0.57	5.7	5.5	0.5	1.0
DN	0.55	5.5	11.8		0.5
VI UP	59.1	591.0	429.0	10.9	1.4
DN	2.5	25.0	39.3		0.6
VII UP	12.7	127.0	82.9	2.3	1.5
DN	2.2	22.0	36.3		0.6

Table VII : Comparison of Dose (MRAD) resulting from ^{22}Na fluence and Toshiba glass measurements.

Positions I and II — Fluences and Doses normalised to 10^{18} protons/run lost at the Lambertson magnets.

Positions III to VII — Fluences and Doses normalised to $4 \cdot 10^{19}$ accelerated protons/run.

Position I — values averaged over runs 1 to 5

Position II, III + VII — values averaged over runs 1 to 7

Positions IV + V — values averaged over runs 2 to 7

Position VI — values averaged over runs 1 to 6.

FIGURE CAPTIONS

Fig. 1 Gives the approximate longitudinal dosimeter positions in the FNAL ring tunnel. Two sets of detectors are exposed at each location:
- close to the machine components
- on the floor underneath the other dosimeter.

Fig. 2 Shows a section from the chart giving the dose rate 1 foot above the ring elements versus z-coordinate in the ring.

Fig. 3 Dimensions of the Lambertson Magnets and details about the dosimeter positions.

Fig. 4 Magnet geometry and dosimeter positions at the A-12 bending magnet.

Fig. 5 Dosimeter positions at the Abort target.

Fig. 6 Dimensions of the special "yellow" magnets used for beam dumping. Cu-coil is replaced by steel.

Fig. 7 The geometrical approximations used in the MAGKA calculations for the dose estimation on the Lambertson Magnets.

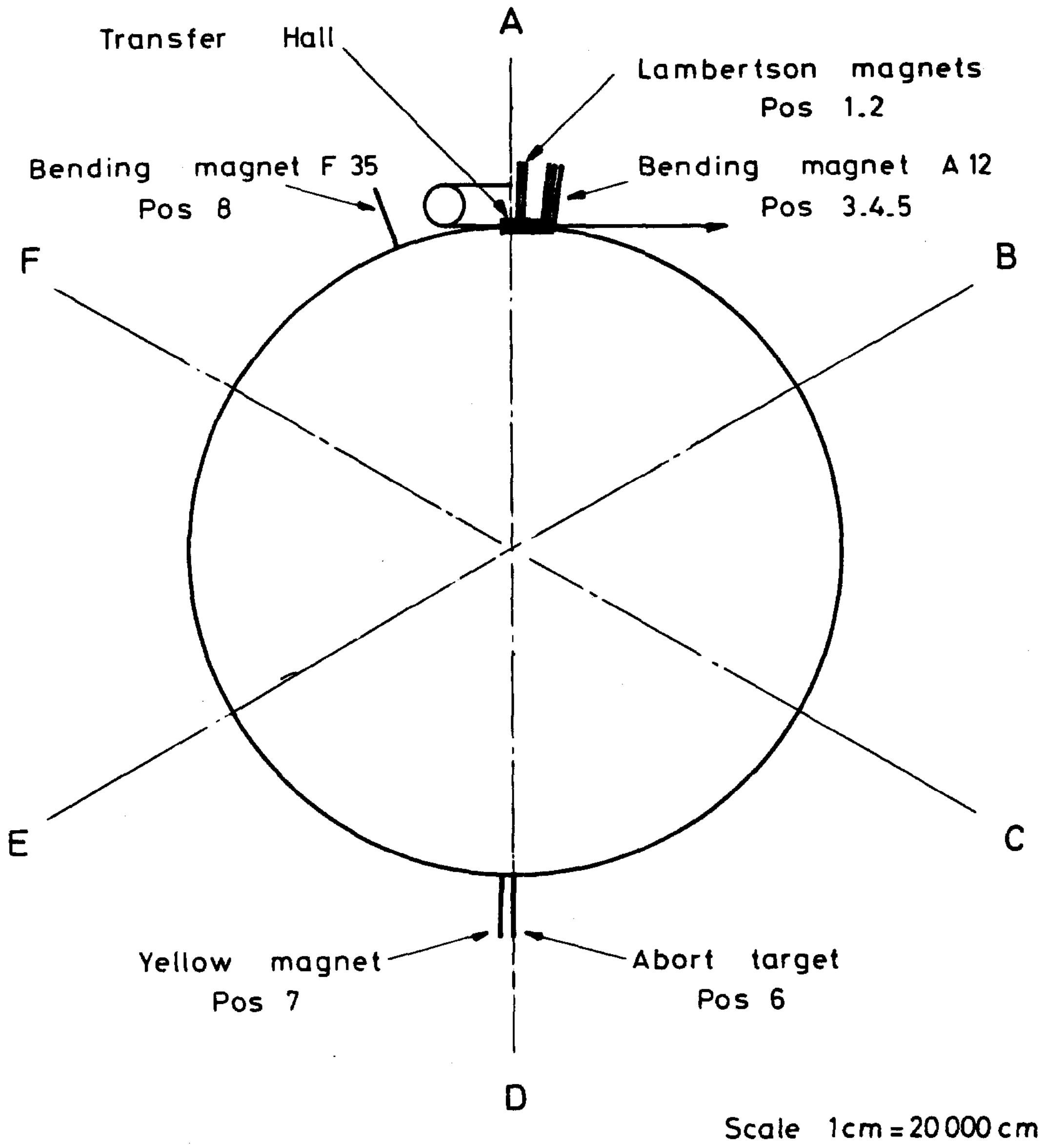

Fig.1 Positions of Dosimeters around NAL Ring

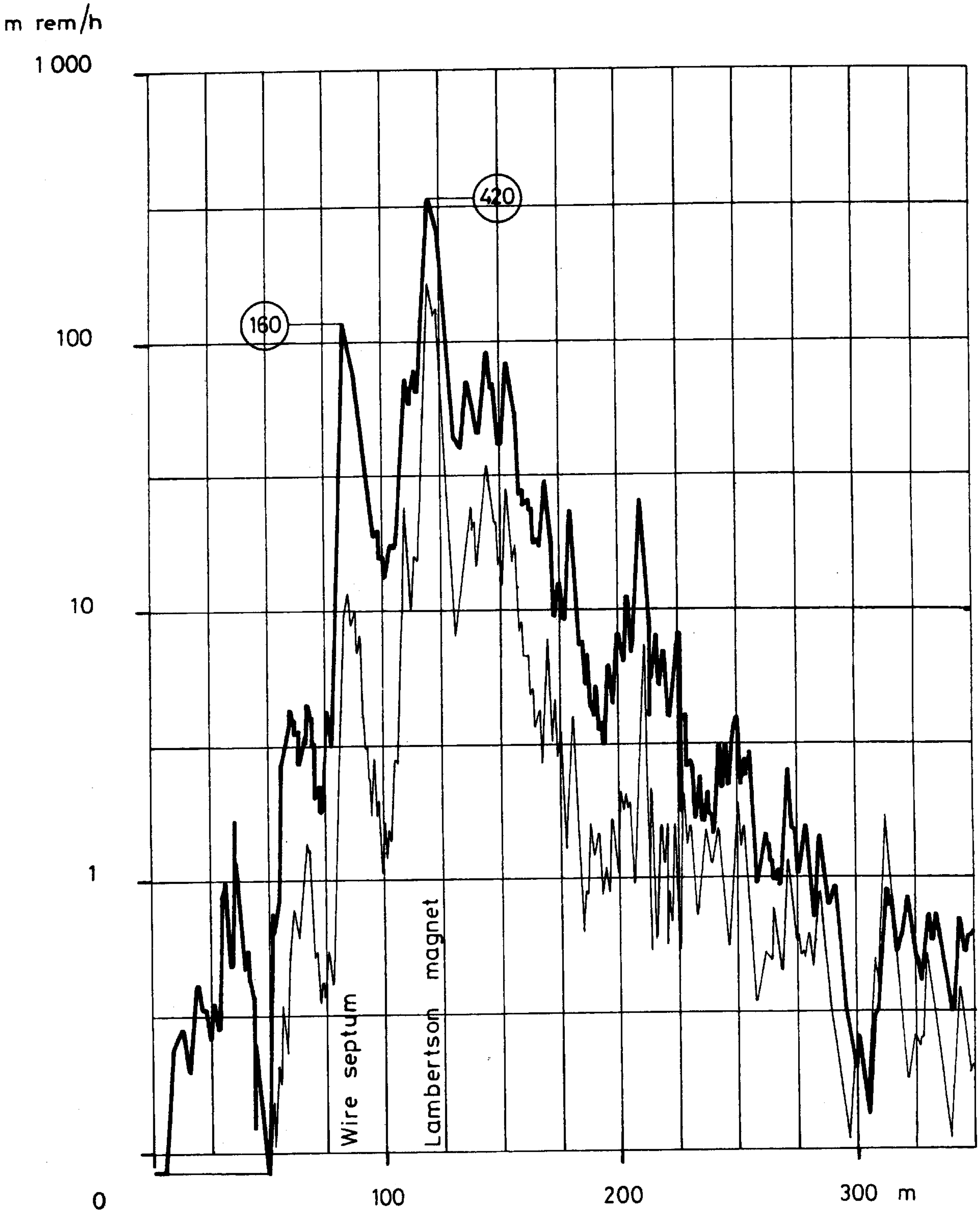

Dose rates measured at NAL 1 foot above magnet

Fig. 2

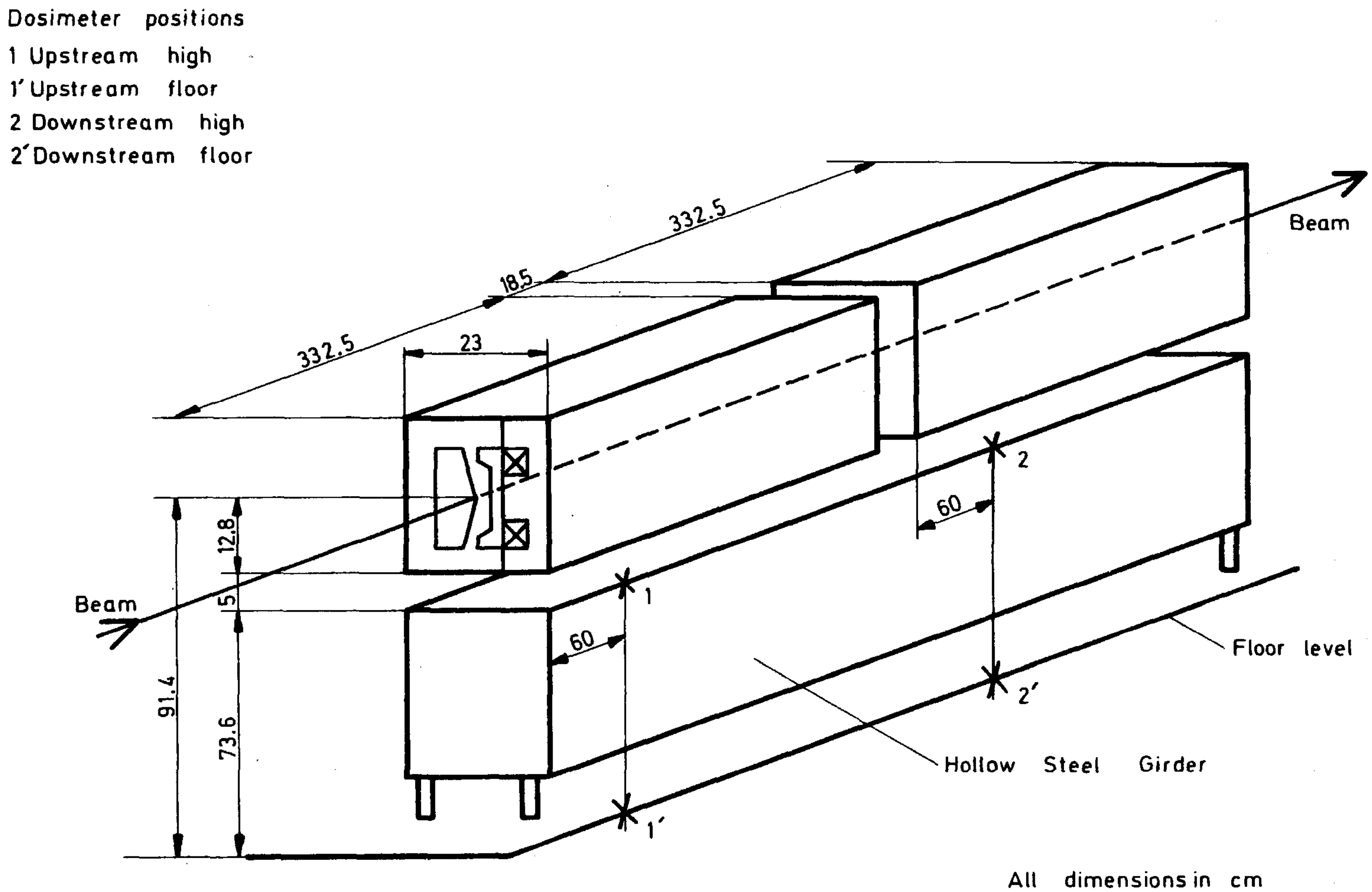

Fig. 3 Dosimeter Positions on the Lambertson Magnets

Dosimeter Positions

3 A 12 Upstream High
3′ A 12 Upstream Floor
4 A 12 Middle High
4′ A 12 Middle Floor
5 A 12 Downstream High
5′ A 12 Downstream Floor

8 F 36 High
8′ F 36 Floor

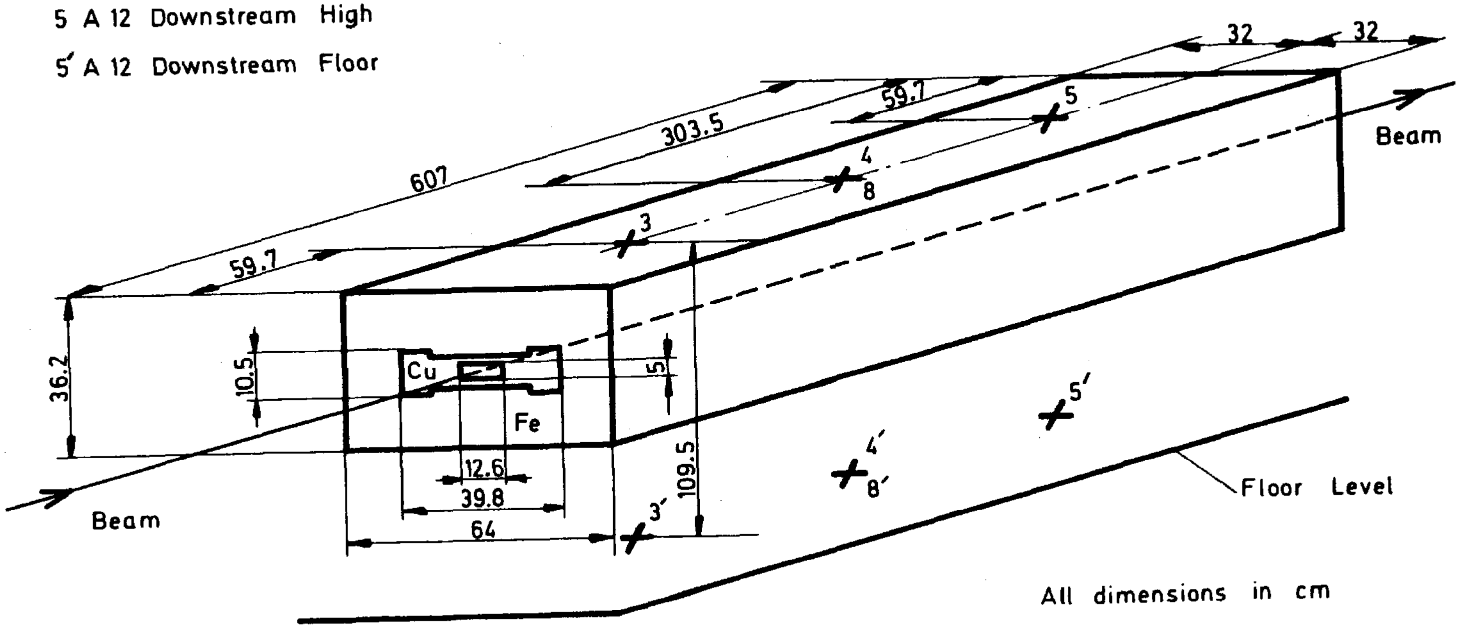

All dimensions in cm

Fig. 4 Dosimeter Positions on Bending Magnets A 12 and F 36

Dosimeter positions

6 Abort Target High

6′ Abort Target Floor

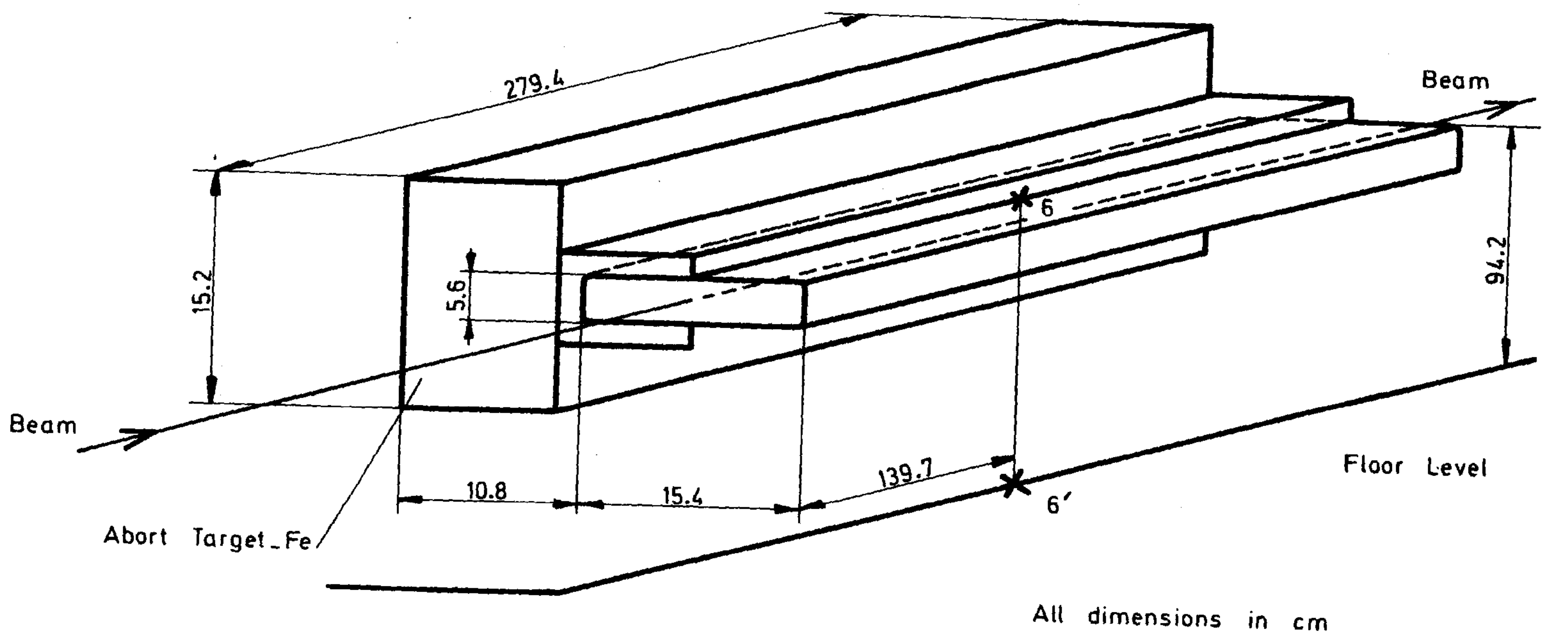

Fig. 5 Dosimeter Positions on the Abort Target

Dosimeter Positions

7 High

7′ Floor

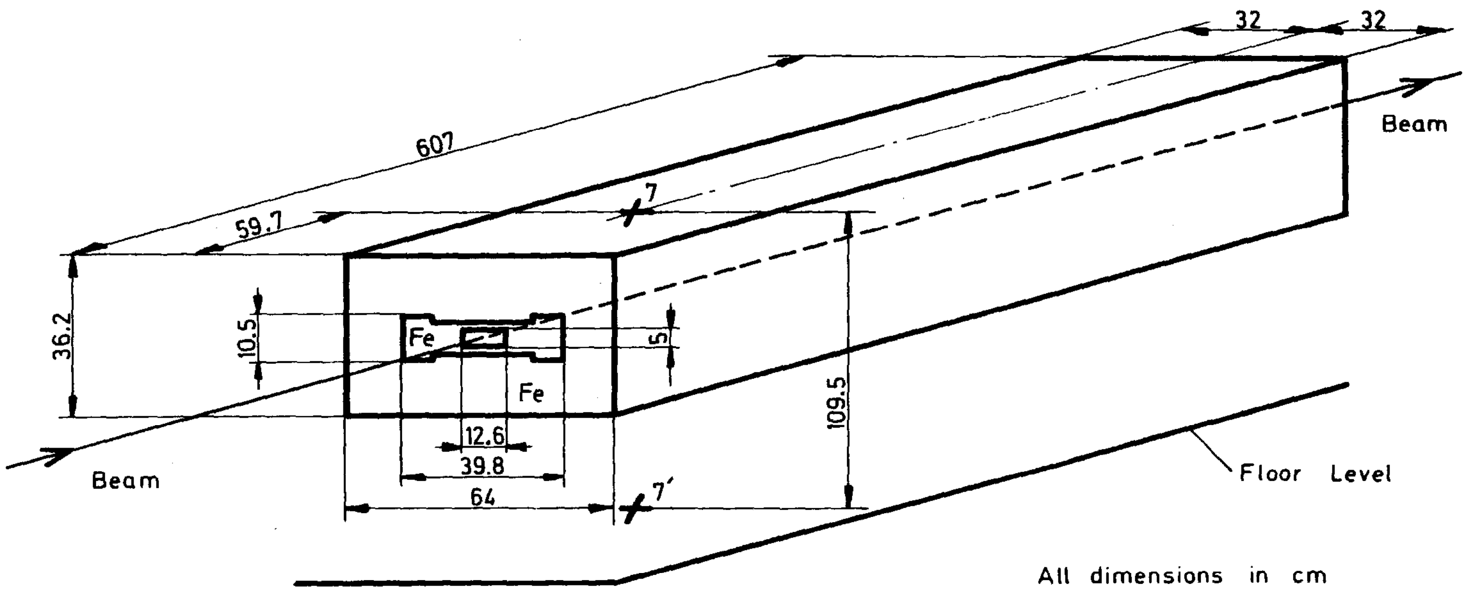

All dimensions in cm

Fig.6 Dosimeter Positions on the Yellow Magnet

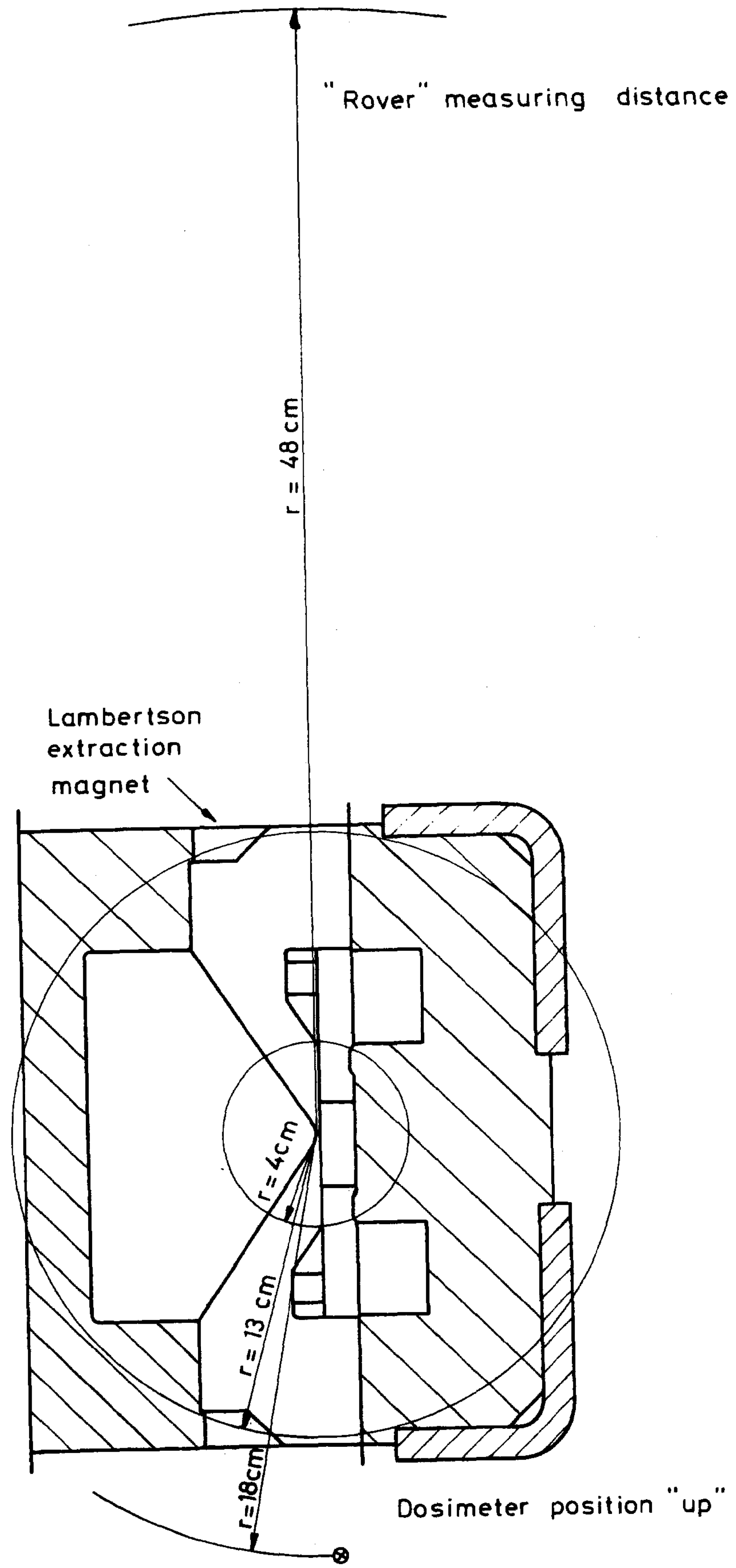

Fig. 7 Geometry for MAGKA – calculations